

Adsorption of Cationic Red X-GRL from Aqueous Solutions by Graphene: Equilibrium, Kinetics and Thermodynamics Study

Y. H. Li,^{a,b,*} T. Liu,^a Q. Du,^a J. Sun,^a Y. Xia,^{a,*} Z. Wang,^a W. Zhang,^c K. Wang,^c H. Zhu,^c and D. Wu^c

^aLaboratory of Fiber Materials and Modern Textile, the Growing Base for State Key Laboratory, Qingdao University, 308 Ningxia Road, Qingdao 266071, China

^bCollege of Electromechanical Engineering, Qingdao University, 308 Ningxia Road, Qingdao 266071, China

^cKey Laboratory for Advanced Manufacturing by Material Processing Technology and Department of Mechanical Engineering, Tsinghua University, Beijing 100084, China

Original scientific paper

Received: August 30, 2011

Accepted: November 18, 2011

Graphene was prepared and used as an adsorbent for removal of cationic red X-GRL from aqueous solutions. The physico-chemical properties of graphene were characterized by the transmission electron microscope (TEM), the Brunauer–Emmett–Teller (BET) specific surface area measurement, atomic force microscope (AFM), and Raman microscope. The adsorption properties of cationic red X-GRL onto graphene were studied as a function of pH, adsorbent dosage, contact time, and temperature. Kinetic data were well fitted by a pseudo second-order model. Langmuir and Freundlich adsorption models were applied to describe the isotherms and isotherm constants. Equilibrium data agreed very well with the Langmuir model. Thermodynamic studies showed that the adsorption was a spontaneous and endothermic process.

Key words:

Graphene, dye, adsorption, kinetics, thermodynamics

Introduction

Wide use of dyes in industries such as textiles, dyeing, electroplating, printing and tanneries leads to large amounts of dye-containing wastewater to be discharged into the environment.¹ Dyes are toxic to human health through their ingestion and to aquatic organisms through both absorption and reflection of sunlight entering the water. Most dyes are non-biodegradable in nature and stable to light and oxidation.² Therefore, excessive dyes should be reduced to a tolerable level before being discharged into drainage systems.

Various physicochemical methods such as coagulation,³ flocculation,⁴ biodegradation,⁵ advanced oxidation,^{6,7} ultrafiltration,⁸ and adsorption^{9–11} have been applied to remove dyes from aqueous solutions. Among them, adsorption has gained increased attention in removing dyes from aqueous solutions due to its simplicity, high efficiency, minimization of chemical sludge, and regeneration of adsorbents. Carbonaceous materials such as activated carbon,¹³ carbon nanotubes¹⁴ and their composites¹⁵ are the most commonly used dye

adsorbents and show excellent dye adsorption capabilities.

Graphene, a new carbon nanomaterial, has unique physical, chemical, electrical and mechanical properties^{16–19} and is suitable for preparing nanodevices and advanced composite materials.^{20–22} Recently, graphene and graphene oxide were used as adsorbents to remove methyl orange,²³ naphthalene,²⁴ 1-naphthol,²⁵ arsenic,²⁶ fluoride,²⁷ Hg²⁺, Pb²⁺, Cd²⁺, and Cu²⁺ from aqueous solutions, and showed high adsorption capacities and fast adsorption rates.^{28–31} To our knowledge, no investigation has been carried on using graphene as an adsorbent to remove cationic red X-GRL from aqueous solutions.

Therefore, the objective of this work was to fully investigate the adsorption behavior of cationic red X-GRL adsorbed by graphene. Cationic Red X-GRL, an azo-dye, was selected for the study because it is toxic, non-biodegradable, and widely used in industries. The influences of parameters such as pH, adsorbent dosage, contact time, and temperature were investigated to increase our understanding of the dye adsorption properties of graphene. Adsorption isotherm, kinetic and thermodynamic studies were carried out to explain the adsorption mechanism.

*Corresponding author. E-mail address: liyanhui@tsinghua.org.cn; xiayzh@qdu.edu.cn. Fax: +86 532 85951842

Experimental

Materials

Graphene oxide was prepared from expandable graphite (Henglide Graphite Co., Ltd, China) by the modified Hummers' method.³² 3 g graphene oxide was dispersed into 1500 mL deionized water and homogeneously scattered by ultrasonic treatment for 30 min. 200 mL hydrazine hydrate solution (30 %) was added into graphene oxide solution. Then the mixture was sealed and heated at 110 °C for 12 h. As the solution pH reached 6.5 after rinsing with deionized water, graphene was filtrated, dried, and stored for further use. Cationic red X-GRL (molecular mass: 356.84 g mol⁻¹) was purified from industrial cationic red X-GRL by extraction with methanol recrystallization method at 50 °C and its molecular structure was shown in Fig. 1. All other reagents were obtained from Sinopharm Chemical Reagent Co. Ltd, China.

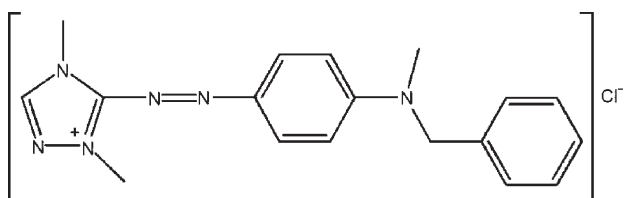


Fig. 1 – Structural formula of cationic red X-GRL

Characterization of graphene

The morphology and structure of graphene was characterized by TEM (JEM-2100F). The BET specific surface area and pore size of graphene were determined from the N₂ adsorption at -196 °C using a Micrometric ASAP 2000 system. Atomic force microscopic (AFM) images were recorded with a Nanoscope IIIa scanning probe microscope (Digital Instruments). Raman spectroscopy was performed with a Renishaw RM2000 Raman microscope.

Batch adsorption experiments

Adsorption experiments were conducted by batch method in stoppered glass conical flasks. Stock solutions (1000 mg L⁻¹) were prepared by dissolving cationic red X-GRL in deionized water. For each time 0.05 g graphene and 100 mL cationic red X-GRL solution were mixed in a flask and then shaken in a thermostat shaker at 150 rpm and room temperature (288 K).

In adsorption isotherm studies, solutions with initial concentrations from 20–140 mg L⁻¹ with a step size of 20 mg L⁻¹ were added, the pH was not

adjusted, and the equilibrium time was set as 24 h to make adsorption reach equilibrium completely. Samples were separated by filtration and cationic red X-GRL concentrations were analyzed by a UV-visible spectrophotometer (TU-1810, Beijing Purkinje Co., Ltd) at λ_{\max} 532 nm. Each experiment was repeated 3 times under identical conditions. The uptake of the adsorbate at equilibrium, q_e (mg g⁻¹), was calculated by:

$$q_e = \left(\frac{\gamma_0 - \gamma_e}{m} \right) V \quad (1)$$

where γ_0 and γ_e were initial and equilibrium concentrations of cationic red X-GRL (mg L⁻¹), respectively, m was the mass of adsorbent (g) and V was volume of the solution (L).

The effect of initial pH on cationic red X-GRL adsorption by graphene was conducted in a pH range of 1.9–10.2. The solution pH was adjusted by adding appropriate concentrations of HNO₃ or NaOH solutions. For every experiment, 100 mL of the solutions with cationic red X-GRL concentrations of 40 and 80 mg L⁻¹ were mixed with 0.05 g of graphene. Experiments were conducted at 288 K, samples were separated and analyzed after 24 h.

The kinetic studies were performed following a similar procedure at 288 K. The solution pH was not adjusted, the initial concentrations of cationic red X-GRL were set as 40 and 80 mg L⁻¹, respectively. The samples were separated at predetermined time intervals. The amount of uptake at time t , q_t (mg g⁻¹), was calculated by:

$$q_t = \left(\frac{\gamma_0 - \gamma_t}{m} \right) V \quad (2)$$

where γ_t (mg L⁻¹) is the concentration of fluoride ions at indicated time.

To evaluate the thermodynamic properties, 0.05 g graphene were added into 100 mL solutions with initial fluoride concentrations ranging from 20 to 140 mg L⁻¹ at a step size of 20 mg L⁻¹. The solution pH was not adjusted. The samples were shaken at 288, 313, and 333 K, respectively, then separated and measured after 24 h.

In order to investigate the regeneration property, graphene after cationic red X-GRL adsorption was collected and washed several times with deionized water and dried at 323 K. Then, the sample was heated at 673 K under H₂ and N₂ atmosphere for 30 min. to burn the chemicals away. The regenerated graphene was used to conduct the adsorption experiments again to test the recycling property of graphene.

Results and discussion

Characterizations of graphene

The structure of graphene was characterized by TEM and shown in Fig. 2. It can be seen that graphene nanosheet is transparent and has clearly flake-like shape. BET analysis shows that the specific surface area of graphene is $305.8 \text{ m}^2 \text{ g}^{-1}$. The average pore size (4V/A by BET) of graphene is 3.63 nm, suggesting that graphene is a mesopore material.



Fig. 2 – TEM image of graphene

From AFM image (Fig. 3a), large graphene sheets are observed. The cross-sectional analysis indicates that the average thickness of graphene is about 1.4 nm (Fig. 3b), indicating that graphene sheets have single or two layers.

Fig. 4 shows Raman spectrum of the graphene. The G peak at 1583 cm^{-1} represents the E_{2g} in-plane vibrational modes. The single and sharp 2D peak appears at 2688 cm^{-1} . The higher intensity of the 2D peak than the G peak indicates the presence of monolayer graphene.³³

Effect of pH

The pH of the solution is one of the most important parameters to affect the adsorption property of an adsorbent in that it governs the degree of ionization of adsorbate and surface charge of the adsorbent.³⁴ Fig. 5 illustrates the effect of the pH of the solution on the adsorption capacity of cationic red X-GRL adsorbed by graphene. It is evident that increasing solution pH significantly increases the adsorption capacity in the pH range from 1.9 to 6.0. The adsorption capacity correspondingly increases from 72.31 and 135.02 mg g^{-1} to 79.85 and 158.70 mg g^{-1} , respectively, or initial cationic red X-GRL concentrations of 40 and 80 mg L^{-1} . At $\text{pH} = 1.9$, the surface charge of graphene is positive and the H^+ ion concentration in solution is high,

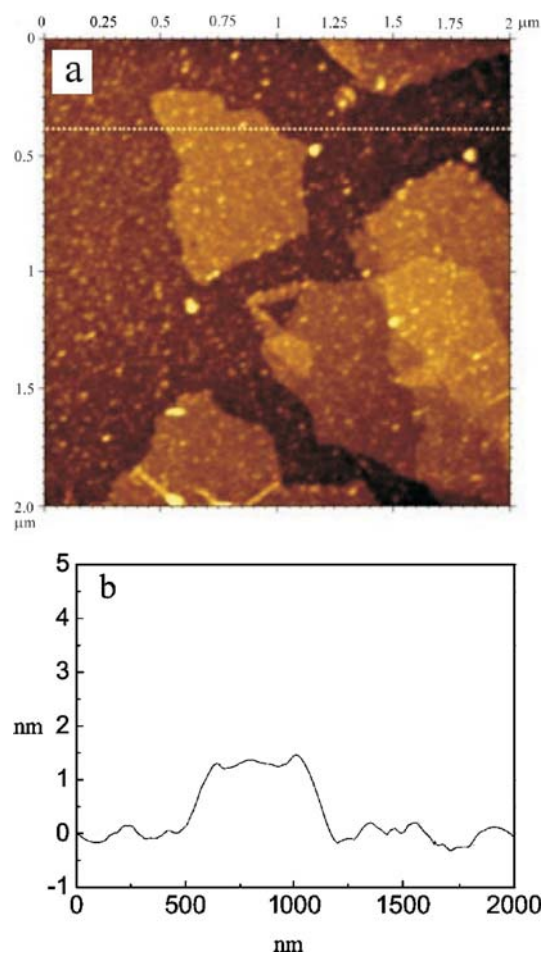


Fig. 3 – AFM images of graphene

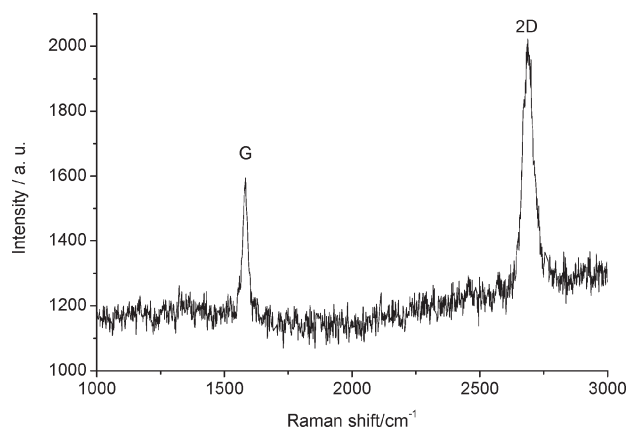


Fig. 4 – Raman spectrum of graphene

competition between H^+ and cationic red X-GRL reduces the adsorbent-adsorbate interaction. Therefore, graphene has the lower adsorption capacity. Increasing solution pH increases the number of hydroxyl groups and negatively charged sites, and the attraction between dye and adsorbent surface,³⁵ thus, adsorption increases with the increase of pH. At $\text{pH} > 5.5$ (pH_{IEP}), graphene surface is negatively charged and the surface functional groups on

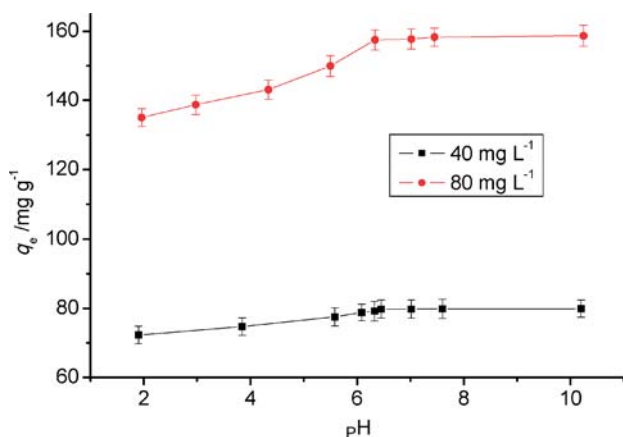


Fig. 5 – The effect of pH on cationic red X-GRL adsorbed by graphene, the error bar represents the standard deviations ($n = 3$)

graphene are deprotonated, which results in a decrease in surface charge density and an enhancement of the adsorption of cationic red X-GRL.³⁶

Graphene is a two-dimensional carbon nanosheet with a single layer of carbon atoms arranged in a honeycomb lattice. For each carbon atom on the lattice, three of the four outer electrons strongly bond with its neighboring atoms by σ orbitals and each carbon atom has a π electron orbit perpendicular to graphene surface, so cationic red X-GRL containing π electrons, can form π - π bonds with graphene and be easily adsorbed by graphene.³⁷

Effect of dosage

The effect of adsorbent dosage on the adsorption capacity of cationic red X-GRL by graphene was shown in Fig. 6. It can be seen that the adsorption capacity of cationic red X-GRL by graphene decreases with increasing dosage. At lower dosage, graphene is separated and dispersed completely in dilute suspensions, all active sites are entirely ex-

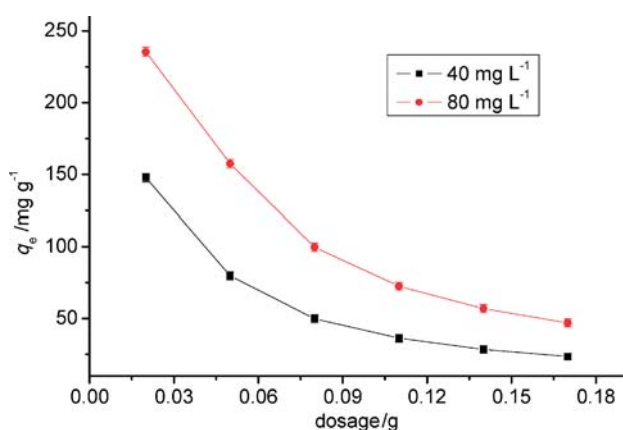


Fig. 6 – The effect of dosage on cationic red X-GRL adsorbed by graphene, the error bar represents the standard deviations ($n = 3$)

posed and the adsorption on the surface is saturated faster, resulting in a higher q_e value. While at higher dosage, high graphene dosage may increase the viscosity and inhibit the diffusion of dye molecules to the surface of graphene.³⁸ At the same time, only parts of active sites are occupied by dye molecules, leading to a lower q_e value. At the same dosage, higher cationic red X-GRL concentration increases the diffusion driving force of dye molecules to transfer in the pores in the adsorbent and raises the contact probability of dye molecules between the aqueous and solid phases, which results in the higher adsorption capacity.

Effect of contact time

The effect of contact time on the removal of cationic red X-GRL by graphene was studied and shown in Fig. 7. A rather fast uptake occurs during the first 3 h of the adsorption process followed by a slower stage as the adsorbed amount of dyes reaches its equilibrium value. The rapid adsorption at the initial contact time is due to the availability of the negatively charged surface of graphene which led to fast electrostatic adsorption of cationic red X-GRL from the solution. When the adsorption of the exterior surface reached saturation, the diminishing availability of the remaining active sites and long range diffusion of the dye molecules entered onto the interior pores of the adsorbent particles make it take a long time to reach equilibrium. Thus, the adsorption rate becomes slower. The equilibrium was found to be nearly 10 h when the maximum dye adsorption capacity was reached.

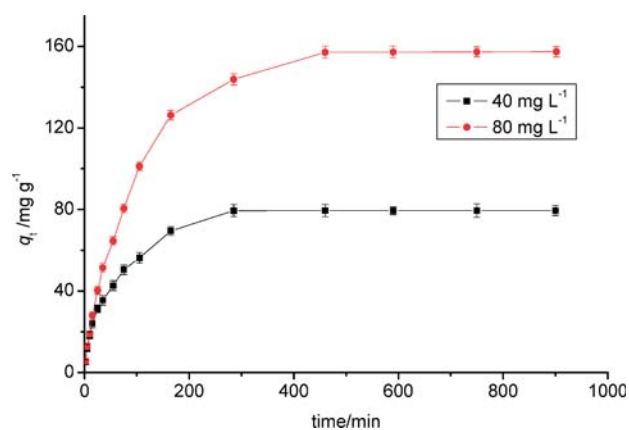


Fig. 7 – The effect of contact time on cationic red X-GRL adsorbed by graphene, the error bar represents the standard deviations ($n = 3$)

Kinetics analysis

The adsorption of adsorbate by an adsorbent in aqueous solution is a phenomenon with complex kinetics. The adsorption rate is strongly influen-

ced by the surface state of the adsorbent and the physico-chemical conditions under which adsorption were carried out. In order to investigate the potential rate controlling steps such as chemical reaction, diffusion control and mass transport processes, four kinetic models, namely, pseudo-first-order, pseudo-second-order, Elovich, and intra-particle diffusion models were analyzed.

The pseudo-first-order equation is expressed as follows:³⁹

$$\log(q_e - q_t) = \log q_e - \frac{k_1}{2.303} t \quad (3)$$

where k_1 is the Lagergren rate constant of adsorption (min^{-1}). The plot of $\log(q_e - q_t)$ vs. t should give a linear relationship from which k_1 and q_e are determined from the slope and intercept of plot, respectively.

Plots of $\log(q_e - q_t)$ vs. t are shown in Fig. 8a. The values of k_1 and q_e were determined from the slope and intercept of linear fitting and listed in Table 1. The lower determination coefficients ($R^2 \leq 0.8775$) suggest that the pseudo-first-order model does not fit well with the experimental data.

The pseudo-second-order model can be represented by the following linear form:⁴⁰

$$\frac{t}{q_t} = \frac{1}{k_2 q_e^2} + \frac{t}{q_e} \quad (4)$$

where k_2 is the pseudo-second-order rate constant of adsorption ($\text{g mg}^{-1} \text{min}^{-1}$). The slope and intercept of the plot of t/q_t vs. t . (Fig. 8b) were used to calculate the values of q_e and k_2 (Table 1).

The determination coefficients of all examined data were found very high ($R^2 \geq 0.9981$). This indicates that the model can be applied for the entire adsorption process and confirms that the adsorption of cationic red X-GRL onto graphene follows the pseudo-second-order kinetic model, indicating that the nature of adsorption is a chemical controlling process.⁴¹

The Elovich model is presented by the following equation:⁴²

$$q_t = \frac{1}{\beta} \ln \alpha \beta + \frac{1}{\beta} \ln t \quad (5)$$

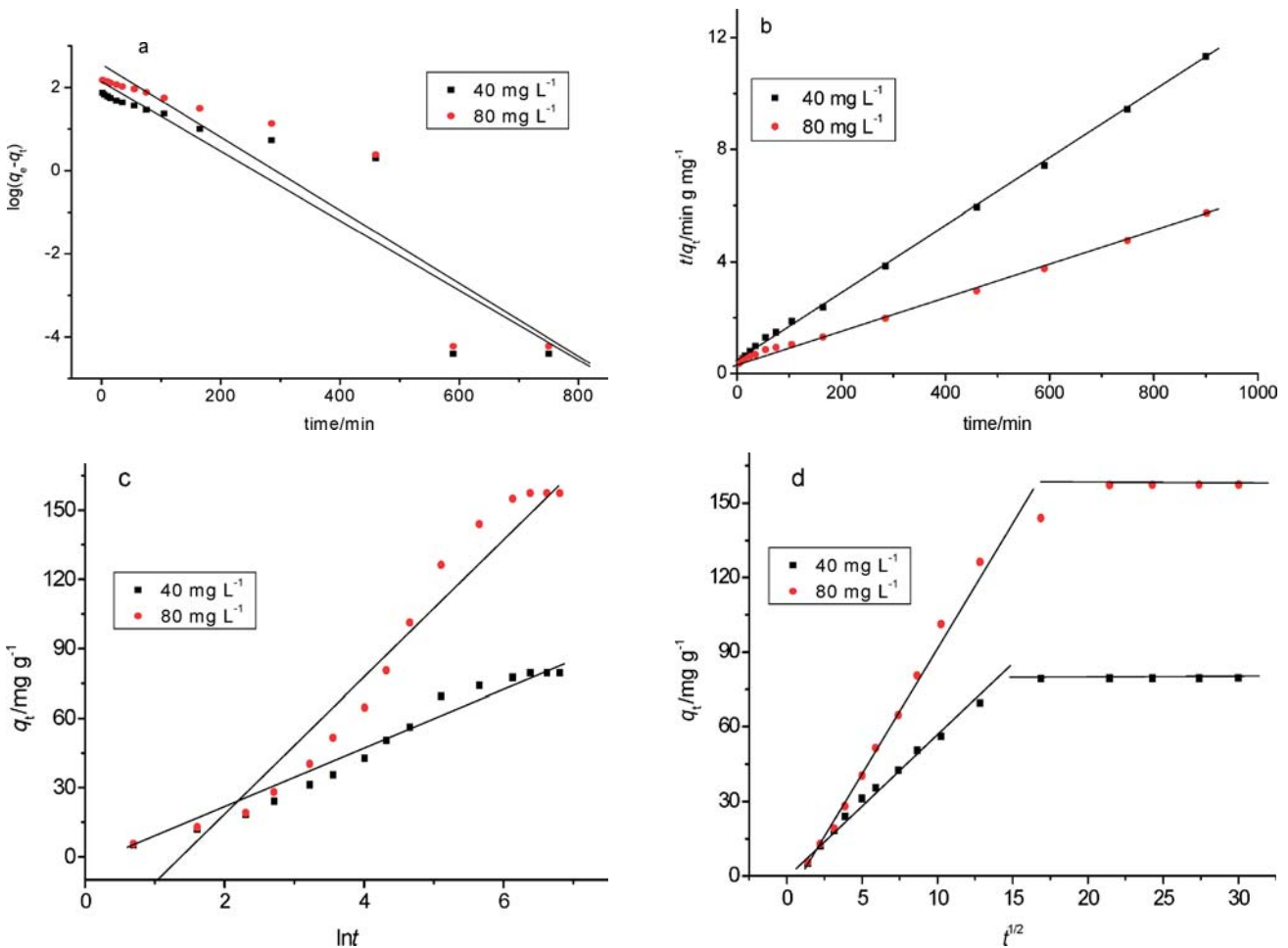


Fig. 8 – Kinetic analysis of cationic red X-GRL adsorbed by graphene: (a) pseudo-first-order model, (b) pseudo-second-order model, (c) Elovich model, and (d) intra-particle diffusion model

Table 1 – Parameters of four kinds of kinetic models

Kinetic model	Parameters	Values	
		40 (mg L ⁻¹)	80 (mg L ⁻¹)
Pseudo-first-order	q_e (mg g ⁻¹)	125.14	310.60
	k_1 (min ⁻¹) · 10 ⁻³	18.88	19.81
	R^2	0.8669	0.8775
Pseudo-second-order	q_e (mg g ⁻¹)	80.03	172.41
	K_2 (g mg ⁻¹ min ⁻¹) · 10 ⁻³	0.29	0.8
	R^2	0.9993	0.9981
Elovich	α	7.33	6.65
	$\beta \cdot 10^{-3}$	32.99	71.54
	R^2	0.9527	0.9765
Intra-particle diffusion	k_1	5.511	8.60 · 10 ⁻³
	R^2	0.9897	0.9957
	k_{11}	9.70	25.00 · 10 ⁻³
	R^2	0.9833	0.9972

where α is the initial adsorption rate (mg g⁻¹ min⁻¹) and β desorption constant (g mg⁻¹). The slope and intercept of the plots of q_t vs. $\ln t$ were used to calculate the values of the constants α and β (Table 1). The values of the determination coefficients obtained from the linear plot of Elovich (Fig. 8c) models are not high ($R^2 \leq 0.9765$), suggesting that the applicability of this model to describe the adsorption processes of cationic red X-GRL onto graphene is unfeasible.

The adsorption mechanism of adsorbate onto adsorbent follows three steps: (1) transport of adsorbate from the boundary film to the external surface of the adsorbent; (2) adsorption at a site on the surface; (3) intra-particle diffusion of the adsorbate molecules to an adsorption site by a pore diffusion process. The slowest of the three steps controls the overall rate of the process. In this study, the adsorption of dye onto graphene takes a long contact time to reach equilibrium. Therefore, it is proposed that the rate of adsorption is governed by the intra-particle diffusion in the pore structure. Weber and Morris model is a widely used intra-particle diffusion model to predict the rate controlling step.⁴³ The rate constants of intra-particle diffusion (k_{id}) at the stage i were determined using the following equation:

$$q_t = k_{id} t^{1/2} + C_i \quad (6)$$

where q_t is the amount of adsorbed dye at time t , $t^{1/2}$ is the square root of the time, C_i is the intercept at stage i . The value of C_i is related to the thickness

of the boundary layer. The larger C_i represents the greater effect of the boundary layer on molecule diffusion. The plots of q_t versus $t^{1/2}$ at different initial dye concentrations show multilinearity characterizations (Fig. 8d), indicating that two steps occurred in the adsorption process. The intra-particle diffusion parameters and the determination coefficients are summarized in Table 1. The first sharp section is the external surface adsorption or instantaneous adsorption stage. The second subdued portion is the gradual adsorption stage, where intra-particle diffusion is rate-controlled. The larger slopes of the first sharp sections indicate that the rate of cationic red X-GRL removal is higher at the beginning stage due to the instantaneous availability of large surface area and active adsorption sites. The lower slopes of the second subdued portion are due to the fact that the decreased concentration gradients cause dye molecule diffusion in the micropores of adsorbent to take a long time, thus leading to a low removal rate.

Adsorption isotherms

Equilibrium study on adsorption provides information on the capacity of the adsorbent. An adsorption isotherm is characterized by certain constant values, which express the surface properties and affinity of the adsorbent, and could also be used to compare the adsorptive capacities of the adsorbent for different pollutants. The adsorption isotherms of cationic red X-GRL onto graphene were studied at 288, 313 and 333 K, and the results are presented in Fig. 9a. The results reveal that the dye adsorption capacity increases with increasing temperature from 288 to 333 K. This may be because the increase in temperature can increase the mobility of the dye molecules as well as produce a swelling effect within the internal structure of graphene, thus enabling the dye molecules to enter into micropores.⁴⁴ Moreover, the increase in temperature may decrease the thickness of the boundary layer surrounding the adsorbents, thus, decrease the mass transfer resistance of adsorbate in the boundary layer.⁴⁵

Equilibrium data can be analyzed using the Freundlich and Langmuir models. The Freundlich model is an empirical equation based on sorption on heterogeneous surface through a multilayer adsorption mechanism.⁴⁵ The linearized form of the Freundlich equation is given as:

$$\ln q_e = \ln k_F + \frac{1}{n} \ln C_e \quad (7)$$

where k_F is the constant indicative of the relative adsorption capacity of the adsorbent and $1/n$ is the constant indicative of the adsorption intensity. The values of k_F and n were calculated by plotting $\ln q_e$

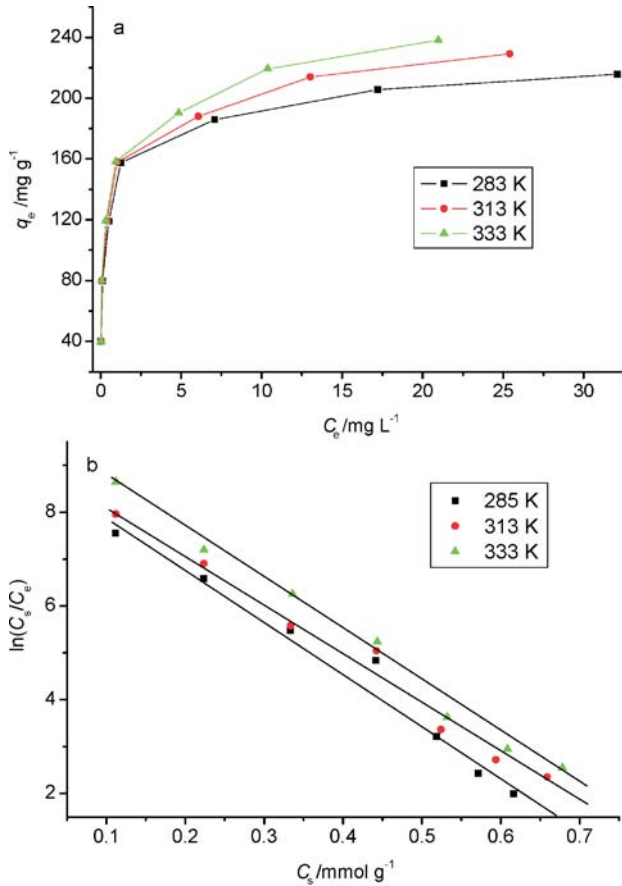


Fig. 9 – (a) Temperature effect on cationic red X-GRL adsorbed by graphene. The error bar represents the standard deviations ($n = 3$), (b) plots of $\ln C_e/C_e$ vs. C_e for calculation of thermodynamic parameters.

vs. $\ln C_e$ and are listed in Table 2. The lower determination coefficients R^2 ($R^2 < 0.9426$) indicate that the adsorption data cannot be fitted by the Freundlich model well.

The Langmuir model is based on the fact that uptake of dye molecules occurs on a homogeneous surface by monolayer adsorption with no interaction between adsorbed molecules, with homogeneous binding sites, equivalent sorption energies, and no interaction between adsorbed species. Its mathematical form is written as:⁴⁷

$$\frac{C_e}{q_e} = \frac{C_e}{q_{\max}} + \frac{1}{q_{\max} k_L} \quad (8)$$

$$K_0 = \frac{a_s}{a_e} = \frac{\nu_s C_s}{\nu_e C_e} \quad (10)$$

where q_{\max} is the maximum adsorption capacity corresponding to complete monolayer coverage (mg g^{-1}) and k_L is a constant indirectly related to adsorption capacity and energy of adsorption (L mg^{-1}), which characterizes the affinity of the adsorbate with the adsorbent. The slope and intercept of the plots of C_e/q_e vs. C_e are used to calculate the values of the constants q_{\max} and k_L .

The good fit of the experimental data and the determination coefficients higher than 0.9966 (Table 2) indicated the applicability of the Langmuir isotherm model. The calculated saturated adsorption capacity reaches 217.39 mg g^{-1} at 288 K.

The essential characteristics of Langmuir dimensionless constant separation factor, R_L , which is given by:

$$R_L = \frac{1}{1 + k_L C_0} \quad (9)$$

where k_L (L mg^{-1}) is the Langmuir constant and C_0 (mg L^{-1}) is the initial dye concentration. The value of R_L indicates the shape of the isotherm to be either unfavorable ($R_L > 1$), linear ($R_L = 1$), favorable ($0 < R_L < 1$) or irreversible ($R_L = 0$).⁴⁸ The R_L values between 0 and 1 indicate favorable adsorption. In the present study, the calculated values of R_L are observed to be in the range 0.0032–0.0234 at all studied temperatures, indicating that the adsorption of cationic red X-GRL onto graphene is favorable.

Adsorption thermodynamic study

Thermodynamic parameters are usually used to determine the adsorption nature. The standard free energy change, enthalpy change and entropy change were calculated to evaluate the thermodynamic feasibility and the spontaneous nature of the adsorption process in the present studies. Thermodynamic parameters can be calculated from the variation of the thermodynamic equilibrium constant K_0 with the change in temperature.⁴⁹ For adsorption reactions, K_0 is defined as follows:

Table 2 – Parameters of Freundlich and Langmuir adsorption isotherm models for cationic red X-GRL adsorbed by graphene

Temperature (K)	Freundlich			Langmuir		
	n	k_F	R^2	q_{\max}	k_L	R^2
288	4.59	118.99	0.9218	217.39	2.09	0.9988
313	4.52	128.05	0.9426	227.27	2.12	0.9974
333	4.37	134.65	0.9249	238.10	2.21	0.9966

where a_s is the activity of adsorbed dye, a_e is the activity of dye in solution at equilibrium, C_s is the amount of dye adsorbed by per mass of graphene (mmol g^{-1}), v_s is the activity coefficient of the adsorbed dye and v_e is the activity coefficient of dye in solution. As dye concentration in the solution decreases and approaches zero, K_0 can be obtained by plotting $\ln(C_s/C_e)$ vs. C_s and extrapolating C_s to zero (Fig. 9b).⁴⁹ A linear regression analysis finds that the straight line fits the data well, the values of K_0 are obtained from the straight line intercept with the vertical axis. The calculated values of K_0 at temperatures of 288, 313, and 333 K are 9.78, 9.23, and 9.07, respectively (Table 3).

Table 3 – Thermodynamic parameters for cationic red X-GRL adsorbed by graphene

Thermodynamic constant	Temperature (K)		
	288	313	333
K_0	9.78	9.23	9.07
ΔG_0 (J mol ⁻¹)	-5445.43	-5805.32	-6127.67
ΔH^0 (J mol ⁻¹)	2568.34	2568.34	2568.34
ΔS^0 (J mol ⁻¹ K ⁻¹)	27.85	26.75	26.12

The average standard enthalpy change (ΔH^0) is obtained from Van't Hoof equation:

$$\ln K_0(T_3) - \ln K_0(T_1) = \frac{-\Delta H^0}{R} \left(\frac{1}{T_3} - \frac{1}{T_1} \right) \quad (11)$$

where T_3 and T_1 are two different temperatures. The calculated value of ΔH^0 is 2568.34 J mol⁻¹.

The adsorption standard free energy changes (ΔG^0) can be calculated according to:

$$\Delta G^0 = -RT \ln K_0 \quad (12)$$

where R is the universal gas constant ($8.314 \text{ J K}^{-1} \text{ mol}^{-1}$) and T is the temperature in Kelvin. The standard entropy change (ΔS^0) can be obtained by:

$$\Delta S^0 = - \frac{\Delta G^0 - \Delta H^0}{T} \quad (13)$$

The thermodynamic parameters are listed in Table 3. Positive values of ΔH^0 suggests that the interaction of fluoride adsorbed by graphene is an endothermic process, which is supported by the increasing adsorption of fluoride with the increase in temperature. The negative values of ΔG^0 reveal the fact that the adsorption process was spontaneous. The positive values of ΔS^0 indicate increased randomness at the adsorbent/solution interface during the adsorption of fluoride onto graphene.⁵⁰

Recycling experiments

The repeated availability is an important factor for an advanced adsorbent, which could significantly reduce the overall cost of the adsorbent. The regeneration experiments show that graphene can be effectively regenerated through heat treatment at 673 K under H_2 and N_2 atmosphere. The adsorption capacity of the regenerated graphene has no obvious change compared with the as-grown graphene, indicating that graphene could be employed repeatedly in dye adsorption.

Conclusions

Graphene has been successfully prepared using a modified Hummers' method. The specific surface area and pore diameter of graphene were $305.8 \text{ m}^2 \text{ g}^{-1}$ and 3.63 nm. The equilibrium data followed the Langmuir model, showing the maximum monolayer adsorption capacity of 317.39 mg g^{-1} at 288 K. The adsorption kinetics were found to be best represented by the pseudo-second-order kinetic model. The mechanism of the adsorption process was explained from the intra-particle diffusion model. The negative ΔG^0 and the positive ΔH^0 indicated the spontaneous and endothermic nature of the adsorption.

ACKNOWLEDGEMENTS

This work was supported by the National Natural Science Foundation of China (50802045 and 20975056), Natural Science, Program of NSFC-JSPS (2111140014), SRF for ROCS, SEM, the Middle-aged and Youth Scientist Incentive Foundation of Shandong Province (BS09018), the Taishan Scholar Program of Shandong Province, and Program for Changjiang Scholars and Innovative Research Team in University (IRT0970), China.

Nomenclature

- C_i – intercept of intra-particle diffusion at stage i
- ΔG_0 – standard free energy change, J mol⁻¹
- ΔH^0 – average standard enthalpy change, J mol⁻¹
- K_0 – thermodynamic equilibrium constant
- k_1 – Lagergren rate constant of adsorption, min⁻¹
- k_2 – pseudo-second-order rate constant of adsorption, $\text{g mg}^{-1} \text{ min}^{-1}$
- k_F – constant of the Freundlich equation
- k_{id} – rate constants of intra-particle diffusion at the stage i
- k_L – constant of the Langmuir equation, L mg⁻¹
- m – mass of graphene added during adsorption process, g
- n – constant of the Freundlich equation

- q_e – adsorption amount per mass of graphene at equilibrium, mg g^{-1}
 q_s – adsorption amount per mass of graphene, mmol g^{-1}
 q_t – adsorption amount per mass of graphene at time t , mg g^{-1}
 R – universal gas constant, $8.314 \text{ J K}^{-1} \text{ mol}^{-1}$
 R_L – parameter relate to the shape of the Langmuir equation
 ΔS^0 – standard entropy change, $\text{J mol}^{-1} \text{ K}^{-1}$
 t – adsorption time, min
 V – volume of solution, L
 v_e – activity coefficient of dye in solution
 v_s – activity coefficient of the adsorbed dye
 α – initial adsorption rate of the Elovich model, $\text{mg g}^{-1} \text{ min}^{-1}$
 a_e – activity of dye in solution at equilibrium
 a_s – activity of adsorbed dye
 β – desorption constant of the Elovich model, g mg^{-1}
 γ_0 – initial concentration of cationic red X-GRL, mg L^{-1}
 γ_e – concentration of cationic red X-GRL at equilibrium, mg L^{-1}
 γ_t – concentration of cationic red X-GRL at time t , mg L^{-1}

References

- Liu, C. H., Wu, J. S., Chiu, H. C., Suen, S. Y., Chu, K. H., *Water Res.* **41** (2007) 1491.
- Wang, L., Zhang, J., Zhao, Z., Li, C., Li, Y., Zhang, C., *Desalination* **254** (2010) 68.
- Szygula, A., Guibal, E., Ruiz, M., Sastre, A. M., *Colloids Surf. A* **330** (2008) 219.
- Mishra, A., Bajpai, M., *Bioresour. Technol.* **97** (2006) 1055.
- Kalyani, D. C., Telke, A. A., Dhanve, R. S., Jadhav, J. P., *J. Hazard. Mater.* **163** (2009) 735.
- Hihara, T., Okada, Y., Morita, Z., *Dyes Pigm.* **75** (2007) 225.
- Ghoneim, M. M., El-Desoky, H. S., Zidan, N. M., *Desalination* **274** (2011) 22.
- Deriszadeh, A., Husein, M. M., Harding, T. G., *Environ. Sci. Technol.* **44** (2010) 1767.
- Luo, P., Zhao, Y., Zhang, B., Liu, J., Yang, Y., Liu, J., *Water Res.* **44** (2010) 1489.
- Rauf, M. A., Shehadi, I. A., Hassan, W. W., *Dyes Pigm.* **75** (2007) 723.
- Doğan, M., Karaoğlu, M. H., Alkan, M., *J. Hazard. Mater.* **165** (2009) 1142.
- Ajayan, P. M., *Chem. Rev.* **99** (1999) 1787.
- Li, Y. H., Du, Q. J., Liu, T. H., Qi, Y., Zhang, P., Wang, Z., Xia, Y., *Appl. Surf. Sci.* **257** (2011) 10621.
- Kuo, C. Y., Wu, C. H., Wu, J. Y., *J. Colloid. Interf. Sci.* **327** (2008) 308.
- Gong, J. L., Wang, B., Zeng, G. M., Yang, C. P., Niu, C. G., Niu, Q. Y., Zhou, W. J., Liang, Y., *J. Hazard. Mater.* **164** (2009) 1517.
- Novoselov, K. S., Geim, A. K., Morozov, S. V., Jiang, D., Zhang, Y., Dubonos, S. V., Grigorieva, I. V., Firsov, A. A., *Science* **306** (2004) 666.
- Navarro, C. G., Burghard, M., Kern, K., *Nano Lett.* **8** (2008) 2045.
- Park, S., Lee, K. S., Bozoklu, G., Cai, W., Nguyen, S. T., Ruoff, R. S., *ACS Nano* **3** (2008) 572.
- Balandin, A. A., Ghosh, S., Bao, W., Calizo, J., Teweldebrhan, D., Miao, F., Lau, C. N., *Nano Lett.* **8** (2008) 902.
- Ang, P. K., Chen, W., Wee, A. T. S., Loh, K. P., *J. Am. Chem. Soc.* **130** (2008) 14392.
- Wang, X., Zhi, L., Mullen, K., *Nano Lett.* **8** (2008) 323.
- Stankovich, S., Dikin, D. A., Dommett, G. H. B., Kohlhaas, K. M., Zimney, E. J., Stach, E. A., Piner, R. D., Nguyen, S. T., Ruoff, R. S., *Nature* **442** (2006) 282.
- Li, N., Zheng, M., Chang, X., Ji, G., Lu, H., Xue, L., Pan, L., Cao, J., *J. Solid State Chem.* **184** (2011) 953.
- Zhao, G., Jiang, L., He, Y., Li, J., Dong, H., Wang, X., Hu, W., *Adv. Mater.* **23** (2011) 39593.
- Zhao, G., Li, J., Wang, X., *Chem. Eng. J.* **173** (2011) 185.
- Chandra, V., Park, J., Chun, Y., Lee, J. W., Hwang, I. C., Kim, K. S., *ACS Nano* **4** (2010) 3979.
- Li, Y. H., Zhang, P., Du, Q., Peng, X., Liu, T., Wang, Z., Xia, Y., Zhang, W., Wang, K., Zhu, H., Wu, D., *J. Colloid. Interf. Sci.* **363** (2011) 348.
- Chandra, V., Kim, K. S., *Chem. Commun.* **47** (2011) 3942.
- Deng, X., Lü, L., Li, H., Luo, F., *J. Hazard. Mater.* **183** (2010) 923.
- Yang, S. T., Chang, Y., Wang, H., Liu, G., Chen, S., Wang, Y., Liu, Y., Cao, A., *J. Colloid. Interf. Sci.* **351** (2010) 122.
- Zhang, N., Qiu, H., Si, Y., Wang, W., Gao, J., *Carbon* **49** (2011) 827.
- Hummers, W. S., Offeman, R. E., *J. Am. Chem. Soc.* **80** (2002) 1339.
- Ferrari, A. C., Meyer, J. C., Scardaci, V., Casiraghi, C., Lazzeri, M., Mauri, F., Piscanec, S., Jiang, D., Novoselov, K. S., Roth, S., Geim, A. K., *Phys. Rev. Lett.* **97** (2006) 187401.
- Garcia-Araya, J. F., Beltran, F. J., Alvarez, P., Masa, F. J., *Adsorption* **9** (2003) 107.
- Lai, C. H., Chen, C. Y., *Chemosphere* **44** (2001) 1177.
- Chen, J. P., Lin, M., *Water Res.* **35** (2001) 2385.
- Wu, T., Cai, X., Tan, S., Li, H., Liu, J., Yang, W., *Chem. Eng. J.* **173** (2011) 144.
- Wu, C. H., *J. Hazard. Mater.* **144** (2007) 93.
- Dogan, M., Alkan, M., Demirbas, O., Ozdemir, Y., Ozmetin, C., *Chem. Eng. J.* **124** (2006) 89.
- Ho, Y. S., McKay, G., *Process Biochem.* **34** (1999) 451.
- Cheng, Z., Liu, X., Han, M., Ma, W., *J. Hazard. Mater.* **182** (2010) 408.
- Shien, S. H., Clayton, W. R., *Soil Sci. Soc. Am. J.* **44** (1980) 265.
- Weber, W. J., Morris, J. C., *J. Santi. Eng. Div. ASCE* **89** (1963) 31.
- Venkat, S. M., Indra, D. M., Vimal, C. S., *Dyes Pigm.* **73** (2007) 269.
- Wawrzkiwicz, M., Hubicki, Z., *J. Hazard. Mater.* **172** (2009) 868.
- Freundlich, H. M. F., *Z. Phys. Chem.* **57** (1906) 385.
- Langmuir, I., *J. Am. Chem. Soc.* **38** (1916) 2221.
- Weber, T. W., Chakraborty, P. K., *J. Am. Inst. Chem. Eng.* **20** (1974) 228.
- Li, Y. H., Di, Z., Ding, J., Wu, D., Luan, Z., Zhu, Y., *Water Res.* **39** (2005) 605.
- Özcan, A., Ömeroğlu, Ç., Erdoğan, Y., Özcan, A. S., *J. Hazard. Mater.* **140** (2007) 173.